



Available online at www.sciencedirect.com

ScienceDirect

Advances in Space Research 57 (2016) 218–233

**ADVANCES IN
SPACE
RESEARCH**
(*a COSPAR publication*)
www.elsevier.com/locate/asr

Swarm kinematic orbits and gravity fields from 18 months of GPS data

A. Jäggi ^{a,*}, C. Dahle ^b, D. Arnold ^a, H. Bock ^a, U. Meyer ^a, G. Beutler ^a,
J. van den IJssel ^c

^a *Astronomical Institute, University of Bern, Sidlerstrasse 5, CH-3012 Bern, Switzerland*

^b *German Research Centre for Geosciences, Telegrafenberg, D-14473 Potsdam, Germany*

^c *Faculty of Aerospace Engineering, Kluyverweg 1, 2629 HS Delft, The Netherlands*

Received 20 July 2015; received in revised form 21 October 2015; accepted 24 October 2015

Available online 28 October 2015

Abstract

The Swarm mission consists of three satellites orbiting the Earth at low orbital altitudes. The onboard GPS receivers, star cameras, and laser retro-reflectors make the Swarm mission an interesting candidate to explore the contribution of Swarm GPS data to the recovery of both the static and time-variable gravity fields. We use 1.5 years of Swarm GPS and attitude data to generate kinematic positions of high quality to perform gravity field determination using the Celestial Mechanics Approach. The generated gravity fields reveal severe systematic errors along the geomagnetic equator. Their size is correlated with the ionospheric density and thus strongly varying over the analyzed time period. Similar to the findings of the GOCE mission, the systematic errors are related to the Swarm GPS carrier phase data and may be reduced by rejecting GPS data affected by large ionospheric changes. Such a measure yields a strong reduction of the systematic errors along the geomagnetic equator in the gravity field recovery. Long wavelength signatures of the gravity field may then be recovered with a similar quality as achieved with GRACE GPS data, which makes the Swarm mission well suited to bridge a potential gap between the current GRACE and the future GRACE Follow-On mission.

© 2015 COSPAR. Published by Elsevier Ltd. All rights reserved.

Keywords: Swarm; GPS high-low SST; Gravity field; Geomagnetic equator; Time-variable gravity

1. Introduction

The Swarm mission was launched on 22 November 2013 into an almost polar low Earth orbit (LEO) to study the dynamics of the Earth's magnetic field and its interactions with the Earth system (Fris-Christensen et al., 2008). It belongs to the series of Earth explorer missions of the European Space Agency (ESA) and consists of three identical satellites. The core instruments of each satellite are the

vector and scalar magnetometers to measure the direction and strength of the Earth's magnetic field. Electrical field instruments, consisting of a thermal ion imager and a Langmuir probe, are used to measure the Earth's electric field. The non-gravitational accelerations acting on the satellites are measured by onboard accelerometers. For the purpose of orbit determination each satellite is equipped with 8-channel dual-frequency Global Positioning System (GPS) receivers (Zangerl et al., 2014). Laser retro-reflectors enable an independent validation of the GPS-derived orbits by Satellite Laser Ranging (SLR). Due to this instrumentation one of the secondary objectives of the Swarm mission is dedicated to measure the Earth's gravity field with the onboard GPS high-low satellite-to-satellite tracking (SST) system.

* Corresponding author. Tel.: +41 31 6318596; fax: +41 31 6313869.

E-mail addresses: adrian.jaggi@aiub.unibe.ch (A. Jäggi), dahle@gfz-potsdam.de (C. Dahle), daniel.arnold@aiub.unibe.ch (D. Arnold), heike.bock@aiub.unibe.ch (H. Bock), ulrich.meyer@aiub.unibe.ch (U. Meyer), gerhard.beutler@aiub.unibe.ch (G. Beutler), J.A.A.vandenIJssel@tudelft.nl (J. van den IJssel).

Level-1B to Level-2 data processing is performed in the frame of the Swarm Satellite Constellation Application and Research Facility (SCARF, Olsen et al., 2013). One of the Level-2 products is the Precise Science Orbit (PSO) product computed at the Faculty of Aerospace Engineering at Delft University of Technology (van den IJssel et al., 2015). It consists of a reduced-dynamic and a kinematic orbit solution. The reduced-dynamic solutions are primarily used to precisely geolocate the magnetic and electric field observations. The kinematic positions may be used for the recovery of the Earth's gravity field. For an independent validation both orbit types are computed by the Astronomical Institute of the University of Bern (AIUB), as well, on a best effort basis in the frame of ESA's Swarm Quality Working Group.

Subsequently the AIUB kinematic positions are used for gravity field recovery in order to investigate the currently achievable quality for static gravity field solutions and to get a first glimpse of the capability of Swarm to recover the largest time-variable signals. Section 2 briefly recapitulates the adopted methods for precise orbit determination and assesses the quality of the Swarm kinematic positions. Section 3 introduces the adopted methods for gravity field recovery and analyzes gravity field solutions derived from the kinematic Swarm positions. Special emphasis is put on the description and removal of systematic errors which are observed along the geomagnetic equator. Section 4 eventually gives an outlook to the determination of precise inter-satellite baseline vectors.

2. Swarm kinematic orbit determination

The final GPS orbits and the high-rate 5-s GPS satellite clock corrections (Bock et al., 2009) from the CODE analysis center (Dach et al., 2009; Dach et al., 2014) are used in this article to perform precise orbit determination (POD) for the entire Swarm constellation. Separately, a reduced-dynamic (Wu et al., 1991) and a kinematic (Švehla and Rothacher, 2005) orbit are generated for each satellite within one processing chain from undifferenced GPS carrier phase tracking data. Both orbit types are determined for 24 h orbital arcs in a batch least-squares adjustment implemented in the Development Version 5.3 of the Bernese GNSS Software (Dach et al., 2007), where reduced-dynamic orbit parameters and kinematic positions, respectively, are estimated together with all other relevant parameters like receiver clock corrections and real-valued carrier phase ambiguities.

Kinematic positions are in the focus of this article. They are determined at the observation epochs of the GPS carrier phase measurements by a precise point positioning (PPP) approach (Zumberge et al., 1997). The kinematic positions are determined in a standard batch least-squares adjustment process of ionosphere-free GPS carrier phase observations together with all other relevant parameters without using any information on LEO dynamics (Švehla and Rothacher, 2005). A band-limited part of the

full covariance matrix of kinematic positions may be efficiently derived in the course of kinematic orbit determination (Jäggi et al., 2011b). Only the matrix elements referring to one epoch are used for an epoch-wise weighting of the kinematic positions in the gravity field determination performed in Section 3.

In the first phase of the Swarm mission all satellites delivered 10-s GPS data. On 15 July 2014 the receiver configuration was changed and since then all Swarm satellites are delivering 1-s GPS data. When expressed in GPS time the actual observation epochs are very close to integer seconds for all satellites (van den IJssel et al., 2015). Therefore, the time tags of the kinematic Swarm positions are very close to integer seconds, as well.

To derive kinematic Swarm center-of-mass positions from the GPS data collected by the Swarm POD antennas, additional external information about the antenna locations is required. Antenna offset vectors, expressed in the respective satellite body-fixed systems, are summarized by van den IJssel et al. (2015). The slowly varying center-of-mass positions, expressed in the respective body-fixed systems, are provided in the daily Swarm accelerometer data files. Attitude information from the onboard star-trackers is used to transform the antenna offset vectors into the inertial frame to relate the center-of-mass position to the antenna position in the orbit determination process.

2.1. Antenna phase center variations

Precise modeling of the antenna phase center location is mandatory to fully exploit the accuracy of the GPS carrier phase measurements. This is particularly true for kinematic solutions, which are free of any constraints imposed by models describing the LEO dynamics, and for the subsequent recovery of the Earth's gravity field (Jäggi et al., 2009b). Because ground calibrations of LEO receiver antennas are often not available or of insufficient quality, e.g., due to the neglect of near-field multipath, an in-flight determination of the Swarm receiver antenna phase center variations (PCVs) is needed. Empirical PCVs are derived in an antenna-fixed coordinate system as bin-wise mean values of GPS carrier phase residuals from Swarm reduced-dynamic orbit determination (Jäggi et al., 2006; Jäggi et al., 2009b). The empirical PCVs are derived in four iteration steps with a resolution of 1° in azimuth and elevation.

In the course of the Swarm mission several versions of Level-1B GPS data were released to the scientific community. GPS data of earlier releases were corrected by PCV maps stemming from ground calibrations. Later on, such corrections were no longer applied as no improvement of the POD performance could be observed. Up-to-date releases of Level-1B GPS data therefore reflect the original GPS data. As a consequence of this change the empirical PCVs are different for the various releases of Level-1B GPS data. Fig. 1 shows the empirical PCVs for all Swarm satellites when derived from GPS data without (top row)

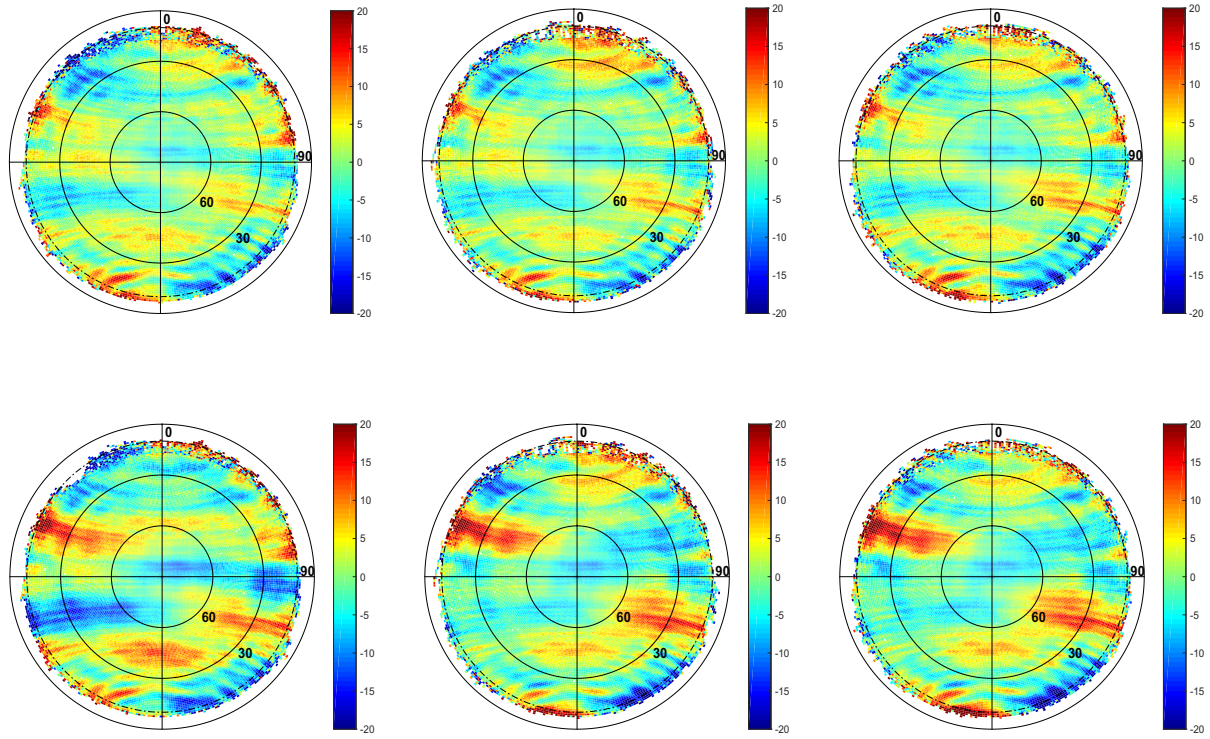


Fig. 1. Empirical PCVs in millimeters for Swarm-A (left column), Swarm-B (middle column), Swarm-C (right column) when using “new” (top row) and “old” (bottom row) GPS carrier phase data. Azimuth 0° nominally points into flight direction.

and with (bottom row) corrections from ground calibration maps, respectively. The two series of GPS data are subsequently denoted by “new” and “old”, respectively. The “old” GPS data files are labeled by ESA with baseline number 03, file counter 01, and creator version 3.11, whereas the “new” GPS data files are labeled with baseline number 03, file counter 02 or higher, and creator version 3.11 or higher. About 100 days of “new” and “old” GPS data from all three satellites are used to generate the empirical PCV maps. To maximize the comparability between the two sets, the PCV maps in the top line are shown before various extensions of the antenna field of view were performed (van den IJssel et al., 2015). Because the Swarm satellites are identical in construction and use the same GPS receivers and antennas, similar PCV maps are expected. This is the case for the PCV maps in the top line of Fig. 1, but not so much for the PCV maps in the bottom line, where pronounced differences between the PCV maps of Swarm-A and Swarm-B can be seen, e.g., for azimuth angles between 180° and 270° . Furthermore, the structures in the top line of Fig. 1 have smaller amplitudes than those in the bottom line, indicating that the corrections from the ground calibrations do not improve the orbit determination performance. Nevertheless, thanks to the in-flight determined PCV maps both sets of resulting orbits show an almost equivalent performance in terms of orbit quality and subsequent gravity field recovery, as shown in the following sections.

2.2. Internal validation

Kinematic positions are computed for all Swarm satellites using both, the “old” and the “new” GPS data, together with the respective PCV maps since their first availability on 25 November 2013. “Old” GPS data were only made available up to 19 October 2014, which marks the end date for the kinematic solutions based on this data. “New” GPS data are available throughout the mission. The kinematic positions up to 31 December 2014 are used for the validation presented here.

Let us first study the root mean square (RMS) errors of the ionosphere-free GPS carrier phase residuals of the kinematic orbit determination. Fig. 2 shows the daily RMS errors for the three Swarm satellites when using the “new”

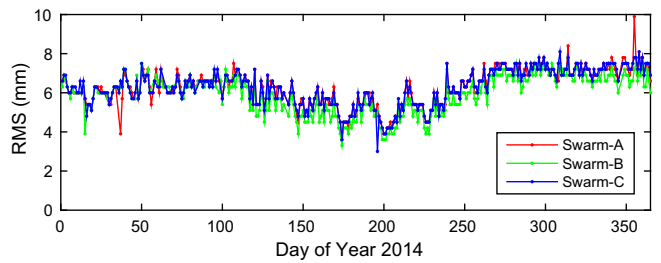


Fig. 2. RMS error of the carrier phase residuals of kinematic orbit determination for all three Swarm satellites in the year 2014.

GPS data. Almost the same curves would be obtained with the “old” GPS data (not shown) thanks to the use of the PCVs from the in-flight calibration described in Section 2.1. Despite taking empirical PCV maps into account, the order of magnitude of the RMS errors shown in Fig. 2 suggests that the overall fit to the GPS data is still considerably worse than that obtained for other LEO receivers, such as those onboard GRACE or TerraSAR-X (Jäggi et al., 2009b). A distinct dependency on the season is moreover observed with smallest RMS errors occurring in the middle of the year. Interestingly, a slightly different behavior of the RMS errors can be seen when the three Swarm satellites were maneuvered to different orbital altitudes in the first quarter of 2014 (see Fig. 1 in van den IJssel et al. (2015) for the evolution of the Swarm orbital altitudes). Smallest RMS errors are obtained for the Swarm-B satellite orbiting the Earth at the highest altitude since then.

Fig. 3 shows the size of the ionosphere-free GPS carrier phase residuals of the kinematic orbit determination for the mid-November–December period of 2014 in terms of RMS errors per geographical $1^\circ \times 1^\circ$ bins. Fig. 3 reveals a clear geographical dependency, as already described by Sust et al. (2014), where significantly larger residuals occur over the geomagnetic poles and where residuals are generally small and of excellent quality outside the high-latitude regions. This geographical dependency is responsible for the daily overall RMS errors from Fig. 2 being considerably larger for Swarm than for other LEO receivers. Note that essentially the same picture is obtained for other time periods (not shown), in particular also in the middle of the year, although with somewhat smaller residuals over the polar regions explaining the dip observed in Fig. 2.

Fig. 3 separates the residuals of the kinematic positioning in ascending (top row) and descending (bottom row) arcs, respectively. For the end of the year 2014 the ascending and descending arcs roughly correspond to a local time

of about 6 h and 18 h at equator crossings, respectively (van den IJssel et al., 2015), which implies a dawn-dusk orbit geometry. This is similar to the GOCE mission, which always had a dusk-dawn geometry. It is interesting to note that similar disturbances are observed as for GOCE (Bock et al., 2014; Jäggi et al., 2015). In particular for the orbital arcs around 18 h, where the satellites are passing an environment of large ionospheric scintillations shortly after dusk (Basu and Groves, 2001), an increased level of the carrier phase residuals is present around the geomagnetic equator, as well. These findings, and the degraded performance observed for gravity field recovery along the geomagnetic equator that will be reported in Section 3.2, motivate to reject the GPS carrier phase observations affected by large ionosphere changes in analogy to the experience from GOCE. Note that higher order ionospheric (HOI) terms are neglected for the Swarm analysis, which is also based on the experience from GOCE (Jäggi et al., 2015), where no significant reduction could be seen when adopting the HOI correction model as recommended by the IERS Conventions 2010 (Petit and Luzum, 2010).

2.3. Removal of problematic GPS data

In analogy to the treatment of the GPS data from the GOCE mission (Jäggi et al., 2015), measurements with large between-epoch changes may also easily be rejected for the Swarm mission by analyzing time-differences of the geometry-free linear combination of the original GPS carrier phase observations. The geometry-free linear combination of the L_1 and L_2 carrier phase observations, i.e., the plain difference of L_1 and L_2 , only contains the ionospheric delay and the initial carrier phase ambiguities such that the analysis of differences between subsequent measurement epochs allows it to reject measurements related to large ionosphere changes over the considered 10-s or

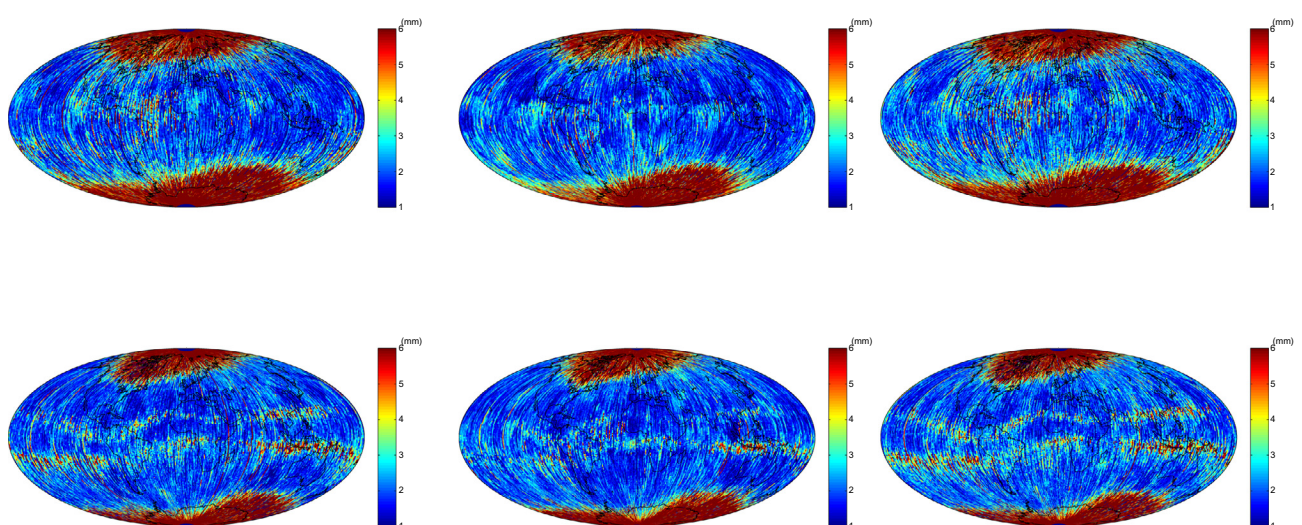


Fig. 3. Global distribution of the bin-wise RMS error of the residuals from kinematic orbit determination of Swarm-A (left column), Swarm-B (middle column), Swarm-C (right column) for ascending (top row) and descending (bottom row) arcs in the period of days 320–365 of the year 2014.

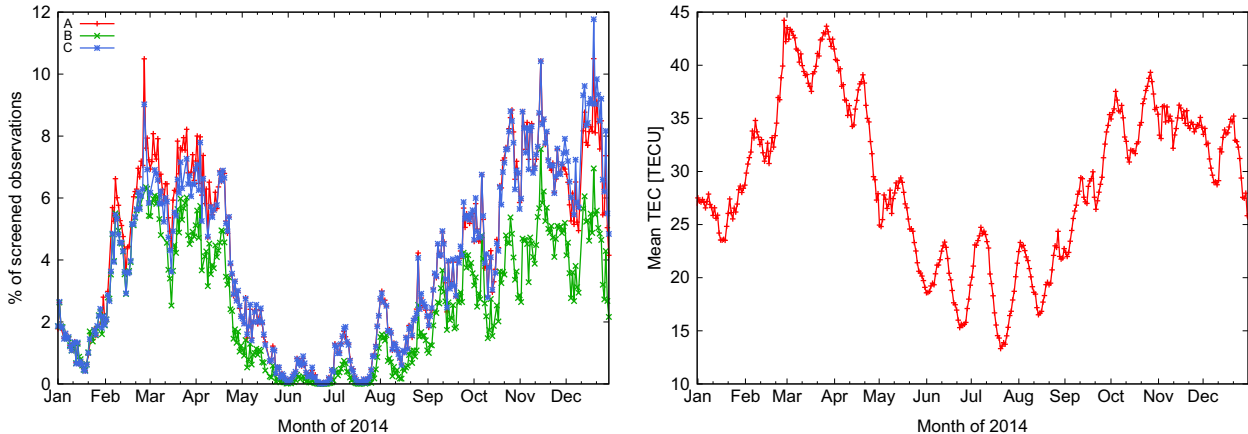


Fig. 4. Percentage of rejected measurements due to large ionosphere changes (left) and mean global total electron content (right).

1-s sampling intervals. Fig. 4 (left) shows the percentage of rejected measurements for all three Swarm satellites when adopting a threshold of a maximally tolerated ionosphere change of 2 cm/s. As opposed to the GOCE mission, where a threshold of 5 cm/s was adopted, a smaller value is needed for Swarm as found by empirical testing, which is an indication that the Swarm GPS receiver is more sensitive to this effect than the GOCE receiver. Using the mentioned thresholds a similar percentage of data is rejected for the two missions due to the ionosphere. Fig. 4 (left) shows that this type of data screening mainly affects the time periods around February–April and September–December. For both periods the ionosphere activity is very high, which is in line with the global mean total electron content shown in Fig. 4 (right) calculated by CODE. In addition the orbital geometry approximately represents a dawn-dusk situation, implying that the descending orbital arcs are passing through an environment of large ionospheric scintillations. Note that the outlined data screening does only marginally affect the months from June to August (Fig. 4, left). Despite that this approximately represents a dusk-dawn orbit situation, there is almost no impact due to a very low ionosphere activity. Fig. 4 (left) also shows a slightly lower rejection rate for Swarm-B after having been maneuvered to the higher orbital altitude.

The outlined screening algorithm is adopted to the “new” GPS data up to 27 May 2015 to compute kinematic positions for the three Swarm satellites. They are subsequently denoted by “screened” positions to distinguish them from the kinematic positions based on the original “new” GPS data, which are subsequently denoted by “unscreened” positions.

2.4. SLR validation

Independent Satellite Laser Ranging (SLR) measurements are used to compare observed ranges between ground stations of the tracking network of the International Laser Ranging Service (ILRS, Pearlman et al., 2002) and the Swarm satellites with computed ranges using

the kinematic solutions. Because the epochs of the kinematic positions usually do not coincide with the epochs of the SLR normal points, neighboring kinematic positions are used to interpolate the kinematic orbit to the epoch of the SLR normal points. Due to obvious differences in the performance of the available SLR stations a subset of high-quality stations is selected to provide a realistic measure of the orbit errors of the Swarm kinematic solutions. These stations (among them well-known sites like Herstmonceux, Graz, Greenbelt, Mount Stromlo, Yarragadee, and Zimmerwald) contribute between 95% and 97% of all available Swarm SLR data and are used for the validation without any further screening and elevation cut-off. A total of about 52,000 normal points is available for Swarm-B up to the end of 2014, but only a much smaller amount of about 24,000 normal points for Swarm-A and Swarm-C, because of the close formation flight of the Swarm-A and Swarm-C satellites rendering the tracking a challenge for the SLR stations. Fig. 5 shows the residuals of the SLR validation of the “unscreened” kinematic Swarm orbits for the time period of 2013 and 2014. The overall statistics yields RMS errors of 3.25, 2.74, and 3.11 cm for Swarm-A, -B, and -C, respectively. Mean offsets are small with values of 0.27, 0.10, and 0.06 cm, respectively. Almost identical validation results are obtained for the kinematic solutions based on the “old” GPS data with RMS errors of 3.25, 2.80, and 3.14 cm for Swarm-A, -B, and -C, respectively.

The SLR validation of the “screened” kinematic Swarm orbits shows very similar mean offsets with values of 0.29, 0.11, and 0.08 cm, for Swarm-A, -B, and -C, respectively, but a degradation of the RMS errors, which read as 3.80, 3.36, and 3.56 cm, respectively. The degradation is mainly caused by a number of outlying passes which are related to weakly determined kinematic positions. Due to the very low degree of freedom, kinematic positioning is very sensitive to the number of GPS satellites used for the epoch-wise estimation of positions and receiver clock corrections. The additional data screening aggravates the situation by further reducing the number of useable satellites per epoch, which is particularly relevant for the Swarm mission. As

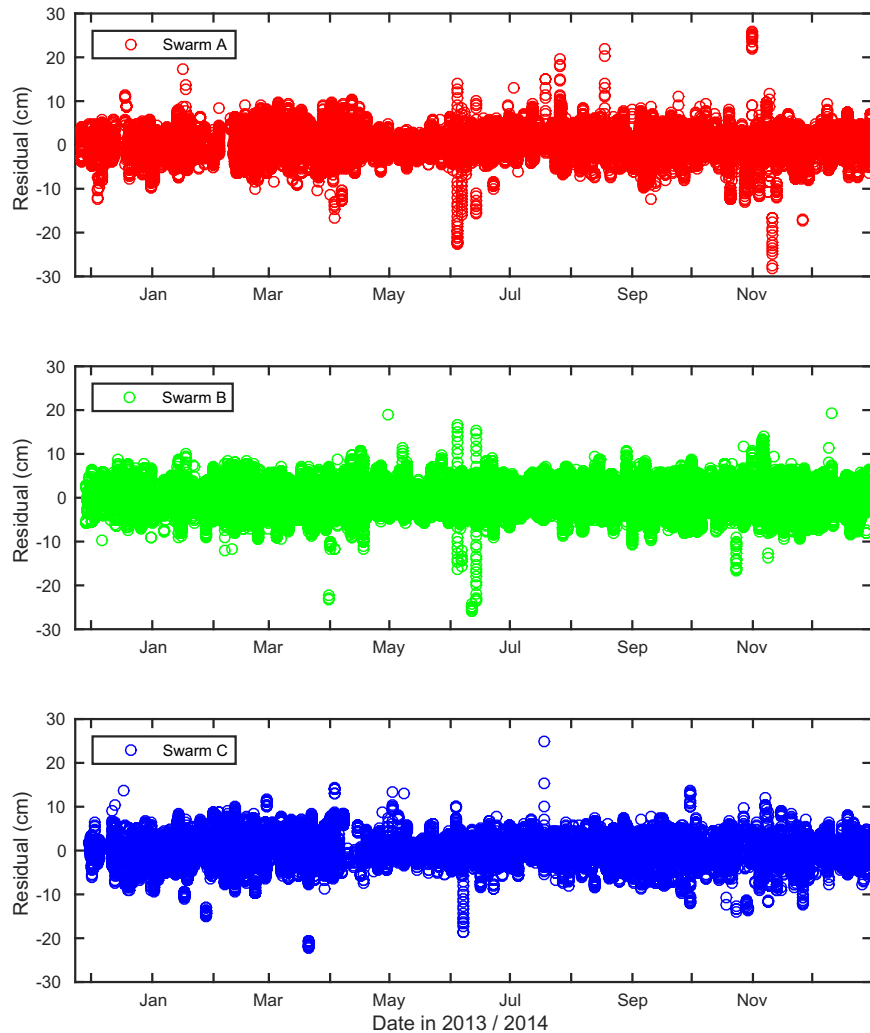


Fig. 5. SLR residuals of the kinematic Swarm orbits.

opposed to the GPS receivers onboard dedicated gravity missions, e.g., GRACE and GOCE which were able to simultaneously track 10 and 12 GPS satellites, respectively, the Swarm receivers provide only 8 channels and therefore track already by default only a relatively small number of satellites. On the other hand, this is fully reflected in the covariance information obtained from the kinematic point positioning, which is used for an epoch-wise weighting of the kinematic positions in the gravity field recovery process. Thanks to the covariance information, degraded kinematic positions due to small number of satellites are automatically down-weighted and have only a minor impact on the resulting gravity field solution.

3. Gravity field determination from Swarm kinematic positions

The Celestial Mechanics Approach is used to solve a generalized orbit determination problem for each Swarm satellite according to the procedure outlined by Jäggi et al. (2011a). In a first step a priori orbits are computed

based on the kinematic positions from Section 2 serving as pseudo-observations. The latter are weighted epoch-wise according to their formal covariance information obtained from the kinematic point positioning and are fitted over 24 h arcs by numerically integrating the equation of motion defined by using the gravity field model EGM2008 (Pavlis et al., 2012) up to different degrees and the ocean tide model FES2004 (Lyard et al., 2006) up to degree 30. Apart from the six Keplerian elements, constant empirical accelerations acting over the entire daily arcs are set up in the radial, along-track and cross-track directions, as well as additional piecewise constant empirical accelerations over 15 min in the same direction. The singularity with the constant accelerations is resolved by constraining the sum of the piecewise constant accelerations to zero in each direction. Swarm accelerometer data were not available in due time to be taken into account for gravity field determination. Non-gravitational accelerations are therefore compensated by empirical accelerations.

Based on the computed a priori orbits gravity field determination from kinematic positions is set up as a

generalized orbit improvement problem (Beutler et al., 2010). The actual orbits are expressed as truncated Taylor series with respect to all unknown parameters, i.e., with respect to the arc-specific orbit parameters (including the empirical accelerations) and the spherical harmonic coefficients, about the a priori orbits. Based on the partial derivatives with respect to all parameters daily normal equations (NEQs) are set up for all parameters according to standard least-squares adjustment. Arc-specific parameters are then pre-eliminated before the daily NEQs are accumulated into NEQs covering longer time spans. The accumulated NEQ matrix is eventually inverted in order to obtain the corrections of the spherical harmonic coefficients with respect to the a priori gravity field coefficients, as well as the associated full covariance information. No regularizations are applied to compute the gravity field solutions presented in this article.

3.1. Comparison of different data sets

Starting on December 1, 2013, the 10-s “unscreened” kinematic positions are used to compute bi-monthly gravity field solutions up to degree and order (d/o) 60, individually for all three Swarm satellites. The higher degrees up to d/o 120 are taken into account using the gravity field model EGM2008 (Pavlis et al., 2012) to reduce omission errors and better reveal potential differences between the individual solutions. The bi-monthly period covering December 2013 and January 2014 is selected because at that time all three satellites were orbiting the Earth at the same altitude before they were maneuvered into different orbits (van den IJssel et al., 2015). The selected period is therefore well suited to compare the quality of the gravity field solutions derived from the data of the individual spaceborne Swarm receivers. Fig. 6 (left) shows the square-roots of degree difference variances of the individ-

ual gravity field recoveries (expressed in geoid heights) with respect to the gravity field model EGM2008. The bi-monthly solutions are almost identical for all three Swarm satellites, indicating that there are no significant differences in the amount and quality of the Swarm kinematic positions. This is in accordance with Fig. 2, which already indicated an almost identical quality of the kinematic positions. The formal errors in Fig. 6 (left) confirm identical observation scenarios for all three Swarm satellites due to similar orbital characteristics at the beginning of the mission. In addition Fig. 6 (left) shows a large discrepancy between the formal errors and the actual differences with respect to superior gravity field models based on GRACE K-Band data. This is not specific for Swarm but was already observed for gravity field recovery from kinematic positions of other LEO missions when not taking empirically derived covariance information into account (Jäggi et al., 2011b).

Fig. 6 (right) shows the square-roots of the degree difference variances of bi-monthly gravity field recoveries with respect to EGM2008 when using “unscreened” kinematic positions of Swarm-C based on the “old” and “new” GPS data, respectively. The almost perfectly coinciding curves illustrate that also from the point of view of gravity field recovery there is almost no difference between the two data sets due to the proper use of the PCVs from the in-flight calibration as described in Section 2.1.

3.2. Impact of data screening

In order to investigate the effect of the ionosphere disturbances described in Section 2.2, the “unscreened” and “screened” kinematic positions of all Swarm satellites are used to compute bi-monthly gravity field solutions. The kinematic positions are used with the maximum available sampling, which is 10-s up to the change of the GPS

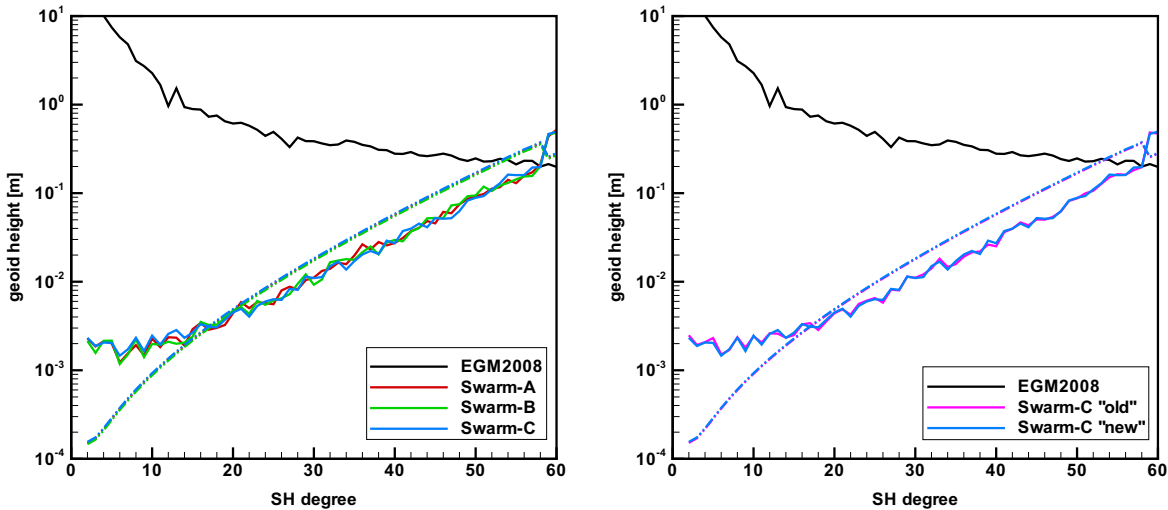


Fig. 6. Square-roots of degree difference variances (solid lines) and error degree variances (dashed lines) of gravity field solutions covering Dec 2013 and Jan 2014 with respect to EGM2008 when using kinematic positions of the individual Swarm satellites (left) and when using “old” and “new” GPS data for the kinematic orbit determination of Swarm-C, respectively.

receiver configuration on 15 July 2014, and 1-s afterwards. The bi-monthly solutions are solved up to d/o 90 by using the a priori gravity field model EGM2008 up to d/o 90, as well. Thereby all NEQs may also be accumulated to compute a long-term static mean field which is independent of the used a priori gravity field model (see Section 3.3). Fig. 7 shows the geoid height differences of the solutions for the periods of March–April, June–July, and November–December 2014 with respect to the gravity field model GOCO05S (Mayer-Gürr et al., 2015) when using “unscreened” (left column) and “screened” (right column)

kinematic positions of all Swarm satellites, respectively. Note that the trends provided by GOCO05S are used to propagate the static part of the field to 01 July 2014 in order to not see secular trends of the Earth's time-variable gravity field in the comparison due to significantly different reference epochs, which is 01 January 2008 for GOCO05S. In addition a Gaussian filter with a radius of 400 km is adopted to focus on the long-wavelength part of the differences. Fig. 7 (left column) shows that the bi-monthly solutions are affected by severe systematic errors along the geomagnetic equator with peak magnitudes of

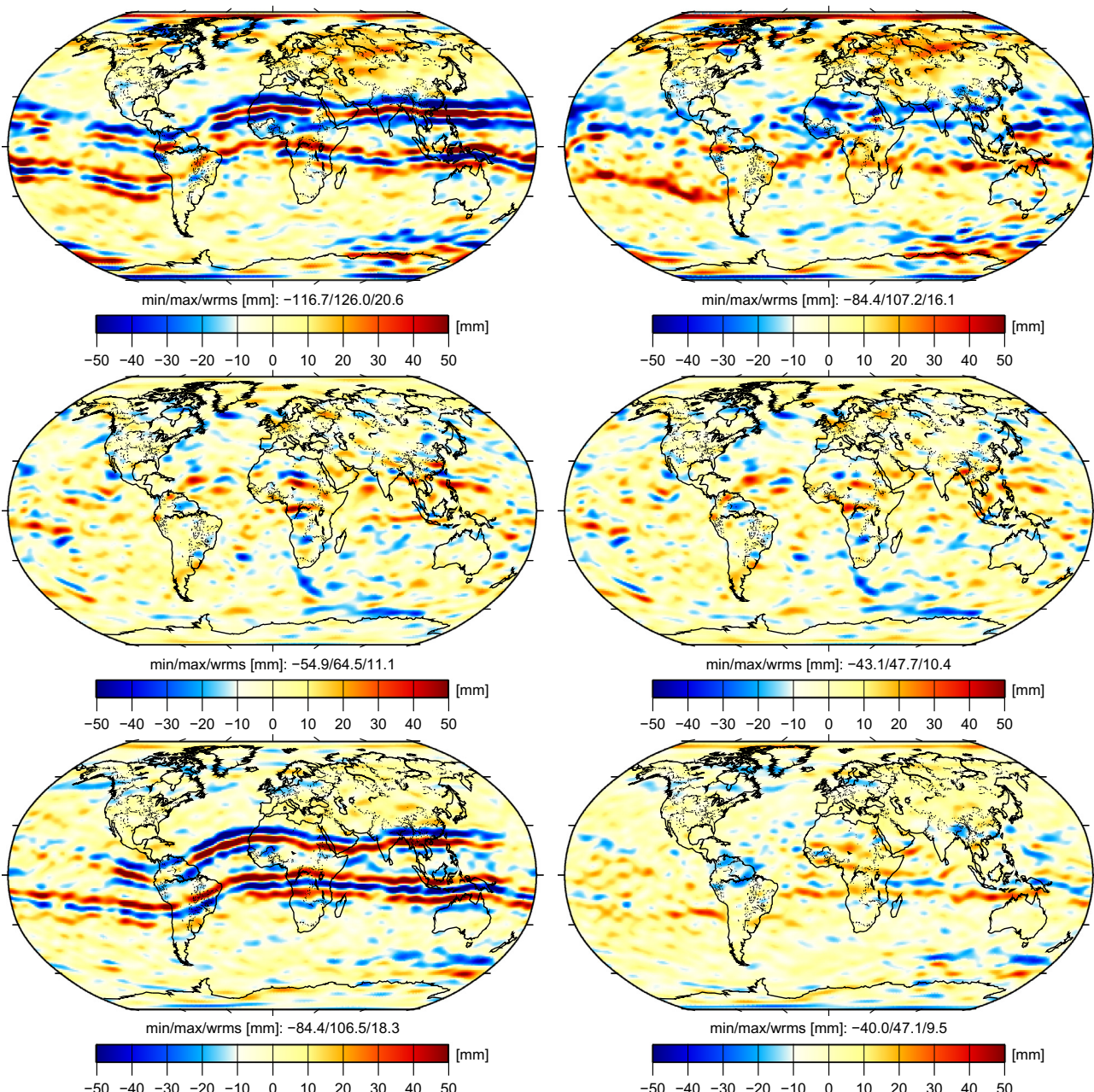


Fig. 7. Filtered geoid height differences of bi-monthly gravity field solutions covering the periods Mar–Apr (top row), Jun–Jul (middle row), Nov–Dec (bottom row) of the year 2014 when using “unscreened” (left column) and “screened” (right column) kinematic positions from all Swarm satellites, respectively. Numerical values indicate minimum, maximum, and weighted RMS errors of geoid height differences with respect to GOCO05S.

more than 10 cm when using the “unscreened” kinematic positions. The systematic errors are very pronounced for the March–April period, then almost disappear for the June–July period, and reappear for the November–December period. The systematic effects are directly linked to the ionosphere activity (see Fig. 4, right) and are therefore strongly varying in magnitude. Fig. 7 (right column) shows that the systematic signatures along the geomagnetic equator may be significantly reduced when using the “screened” kinematic positions, instead. The adopted screening procedure works particularly well for the Nov–Dec period, where GPS data is available with 1-s GPS sampling. For the March–April period, where GPS data is only available with 10-s sampling, a reduction of the systematic errors is achieved, as well, but it is less pronounced than for the November–December period. The lower GPS data sampling makes it obviously more difficult to achieve a similar screening level. At present the threshold of 2 cm/s was simply multiplied by a factor of ten to 20 cm/10-s to screen 10-s data, which might need to be refined. For the June–July period the additional GPS data screening has almost no impact as already predicted by Fig. 4 (left).

Fig. 8 shows the square-roots of the degree difference variances of the bi-monthly solutions of March–April and November–December 2014 with respect to GOCO05S when using “unscreened” and “screened” kinematic positions of all Swarm satellites. Similar to the geoid height differences of Fig. 7, there is a clear and significant reduction of the differences for the March–April and November–December period when using “screened” kinematic positions, but there is no impact on the differences for the June–July period (not shown). The artificial “bumps” seen in the solutions covering periods with high ionosphere activity are mostly eliminated, yielding differences following a straight line for degrees above degree 15. A small degradation is introduced, however, in the long wavelength

part for degrees below 15 when using the “screened” kinematic positions. Most probably the degradation is related to the loss of kinematic positions caused by the additional screening of the GPS data, which is also reflected in the formal errors. A more refined screening therefore needs to be developed to further minimize the amount of rejected GPS data. Note that the differences of the formal errors between Fig. 8 (left) and (right) is primarily related to the 10-s and 1-s sampling of the underlying kinematic positions, respectively.

3.3. Static solutions

Starting on 1 December 2013 the Swarm “unscreened” and “screened” kinematic positions are used to compute long-term gravity field solutions based on data up to 31 December 2014 (13 months) and 27 May 2015 (18 months), respectively. Fig. 9 (left) shows the square-roots of the degree difference variances of the 13 months solution with respect to GOCO05S (evaluated on 01 July 2014) when using “unscreened” and “screened” kinematic positions of all Swarm satellites, respectively, as well as the 18 months solution with respect to GOCO05S (evaluated on 01 September 2014) when using “screened” kinematic positions only. Similar to the findings of Section 3.2, the use of “screened” kinematic positions has a major impact on the quality of the computed gravity field solution. Especially the artificial “bumps” seen in the differences are greatly reduced. As opposed to the bi-monthly solutions shown in Section 3.2, the additional screening of the GPS data does not degrade the quality of the very low degree coefficients of the static solutions due to the larger amount of data also covering periods of quiet ionosphere conditions. The difference curves of the solutions based on the “screened” and “unscreened” kinematic positions coincide up to degree 5 and are superior for the higher degrees when using

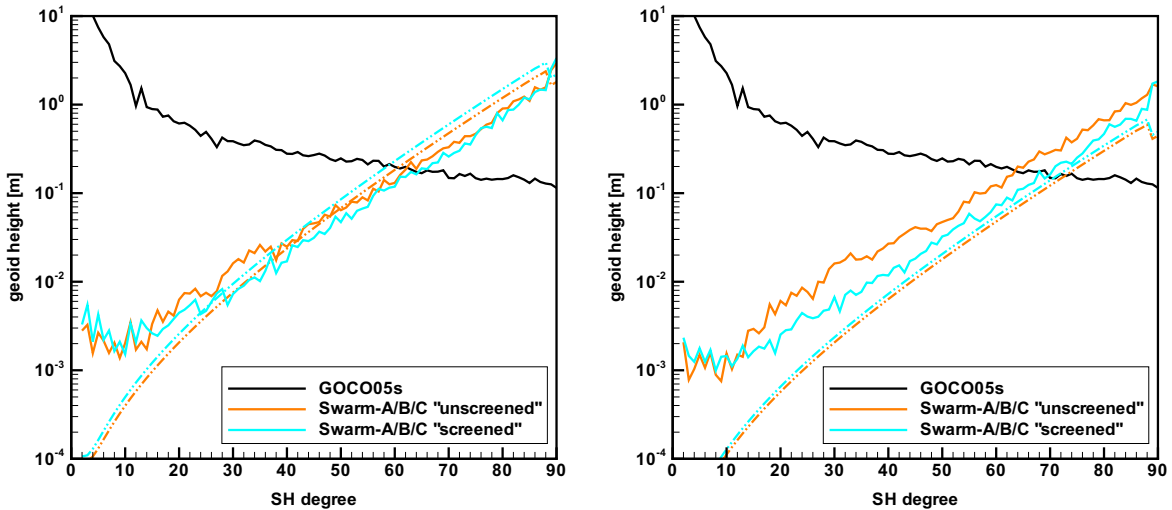


Fig. 8. Square-roots of degree difference variances (solid lines) and error degree variances (dashed lines) of bi-monthly gravity field solutions covering the periods Mar-Apr (left) and Nov-Dec (right) of the year 2014 with respect to GOCO05S when using “unscreened” and “screened” kinematic positions of all three Swarm satellites, respectively.

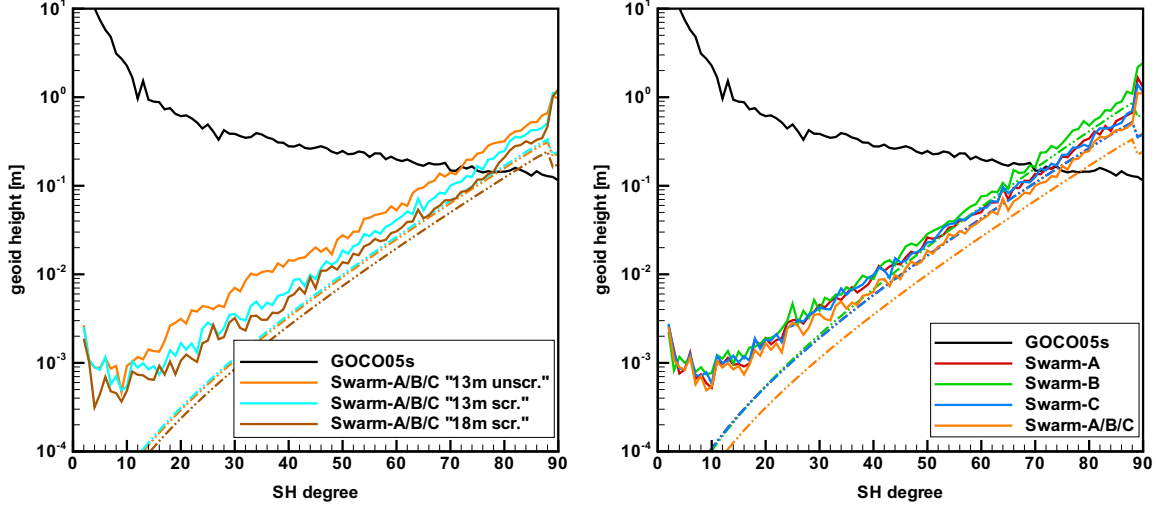


Fig. 9. Square-roots of degree difference variances (solid lines) and error degree variances (dashed lines) of static gravity field solutions with respect to GOCO05S when using different sets and amounts of kinematic positions (left) and individual Swarm satellites (right).

the “screened” kinematic positions. Fig. 9 (left) additionally includes the 18 months solution to indicate that the further accumulation of additional data improves the differences almost over the entire spectral range.

Fig. 9 (right) details the contributions of the individual Swarm satellites to the combined 13 months solution shown in Fig. 9 (left). As expected, the solutions based on Swarm-A and Swarm-C are very similar due to the essentially identical orbit configuration, whereas the solution based on Swarm-B is slightly inferior due to the higher orbital altitude over the major part of the underlying time period used. The effect of the altitude is reflected in the slightly larger slope of the difference curves, which becomes most obvious at the higher degrees, but also in the formal errors.

Fig. 10 eventually shows the geoid height differences (400 km Gauss filtered) of the 13 months solutions with respect to the gravity field model GOCO05S when using “unscreened” and “screened” kinematic positions, respec-

tively. The figure confirms that the artificial signatures along the geomagnetic equator are greatly reduced when using “screened” kinematic positions, improving the weighted RMS error of the filtered geoid height differences from 10 to 6 mm. A further reduction of the weighted RMS error to 4 mm is eventually obtained for the 18 months solution (not shown).

3.4. Comparison with GRACE

In order to assess the currently achieved quality of the static Swarm gravity field solutions, a comparison with corresponding recoveries based on GRACE GPS data is performed. For this purpose only the lower pair of the Swarm constellation is used (Swarm-A and Swarm-C) to generate static Swarm gravity field solutions which are comparable to the extent possible to solutions based on kinematic positions of the two GRACE satellites. For both solutions the one-year period from December 2013 up to

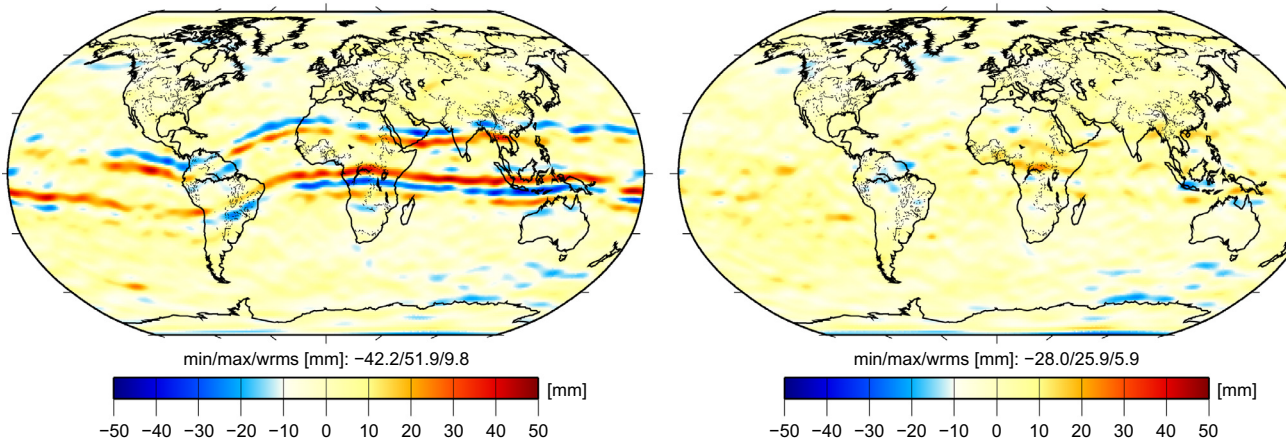


Fig. 10. Filtered geoid height differences of 13 months gravity field solutions when using “unscreened” (left) and “screened” (right) kinematic positions, respectively.

November 2014 is selected. Note that changing PCV maps of the GRACE antennas have to be taken into account in the considered time interval. Due to the GRACE satellite swap in mid 2014, the GRACE-A occultation antenna was activated up to 27 July 2014, whereas the GRACE-B occultation antenna was activated from 28 July 2014 onwards (up to the next satellite swap on 15 December 2014). If not taken into account by a proper antenna in-flight calibration, significantly degraded gravity field recoveries would result (Jäggi et al., 2009b). Fig. 11 compares the square-roots of the degree difference variances of the Swarm solution based on “screened” kinematic positions with respect to GOCO05S (evaluated on 01 July 2014) with the 12 months solution based on kinematic positions of the GRACE satellites. Fig. 11 shows that the differences with respect to GOCO05S are very similar for the long wavelength part of the spectrum up to about degree 20, indicating that Swarm is equally well suited to derive long wavelength time-variable gravity field signals as from GRACE GPS high-low SST observations. For degrees above 20, however, the GRACE solution outperforms the Swarm solution. To a minor extent this is related to the higher orbital altitude of the Swarm satellites, as indicated by a slightly larger slope of the Swarm formal errors. More importantly, however, the Swarm kinematic orbits are overall governed by a larger noise caused by ionosphere related problems over the polar regions and the smaller number of receiver channels than the GRACE kinematic positions (see Section 2.2). This is the main reason that the differences of the Swarm gravity field solution with respect to GOCO05S are worse than for the GRACE solution above degree 20, where the differences between the solutions are largely dominated by the noise of the

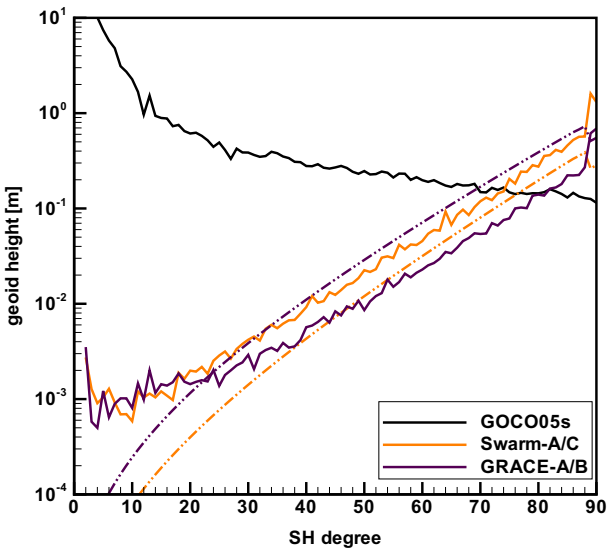


Fig. 11. Square-roots of degree difference variances (solid lines) and error degree variances (dashed lines) of static gravity field solutions with respect to GOCO05S when using 12 months of GRACE-A/B and 12 months of Swarm-A/C kinematic positions, respectively.

kinematic positions. Note that the formal errors of the Swarm and GRACE solutions show a different “ranking”, which is related to the 10-s/1-s and 30-s sampling used for the kinematic positions of Swarm and GRACE, respectively.

Geoid height difference plots of the presented GRACE gravity field solution (not shown) do not reveal artificial signatures along the geomagnetic equator, even if no ionosphere-based GPS data screening is adopted. This is as opposed to Swarm and suggests that either the GRACE GPS data is not affected by ionosphere disturbances or that problematic GPS data is not collected by the GRACE onboard BlackJack GPS receivers (Dunn et al., 2003). To shed further light on this, Figs. 12 and 13 first compare the number of available kinematic positions for GRACE-B and Swarm-A geographically for the time period of March 2014, where the nodes of the two satellites happened to be separated by about 180°. At that time the descending orbital arcs of Swarm-A were passing through the environment of large ionospheric scintillations shortly after dusk, whereas the same was the case for the ascending arcs of GRACE-B. Figs. 12 and 13 indicate that indeed also the kinematic GRACE-B positions are affected by ionosphere-related problems in the sense that a significant part of the positions of the ascending arcs is missing along the geomagnetic equator. A different behavior is observed for Swarm-A, where no systematically missing kinematic positions are observed in the equatorial regions for the descending arcs, but over the polar regions instead. To further confine the origin of the different behavior of the two missions, Fig. 14 shows geographically for both satellites and all arcs the number of GPS observations that are already missing in the original Level-1B RINEX files on both frequencies. Whereas not a single loss is present in the GPS data collected by Swarm-A in the equatorial regions, a rather incomplete situation is seen in the polar regions. Note that equatorial GPS data losses may occasionally also be observed on Swarm (Buchert et al., 2015), but their appearance does not necessarily seem to be correlated with the large ionosphere scintillations as occurring in March 2014. For GRACE-B, however, the situation is completely different. Pronounced gaps are revealed along the geomagnetic equator, explaining that the critical GPS data is simply not present in the Level-1B RINEX files and thus also not affecting the kinematic positioning and the subsequent gravity field recovery. Because the GRACE Level-1B GPS data are not original but pre-processed data (Wu et al., 2006), original Level-1A RINEX files of March 2014 were analyzed, as well. The analysis confirmed that the gaps in the GPS data along the geomagnetic equator are indeed already present to a large extent in the original Level-1A data files (not shown). Only those data gaps which are randomly spread all over the globe in Fig. 14 (right) are not yet present in the original GRACE Level-1A GPS data files and are thus the result of the adopted pre-processing for the Level-1A to Level-1B conversion.

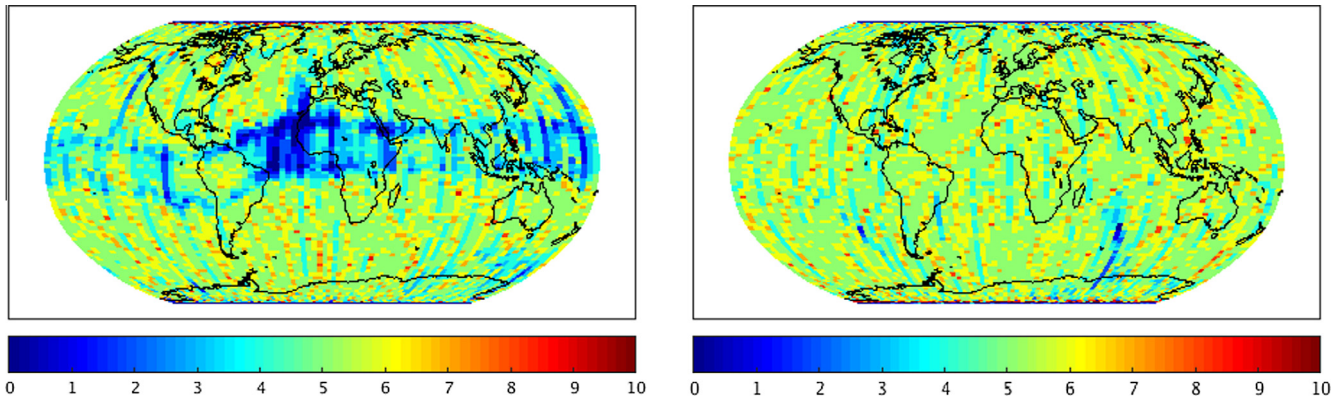


Fig. 12. Number of kinematic GRACE-B positions for ascending (left) and descending (right) arcs in March 2014.

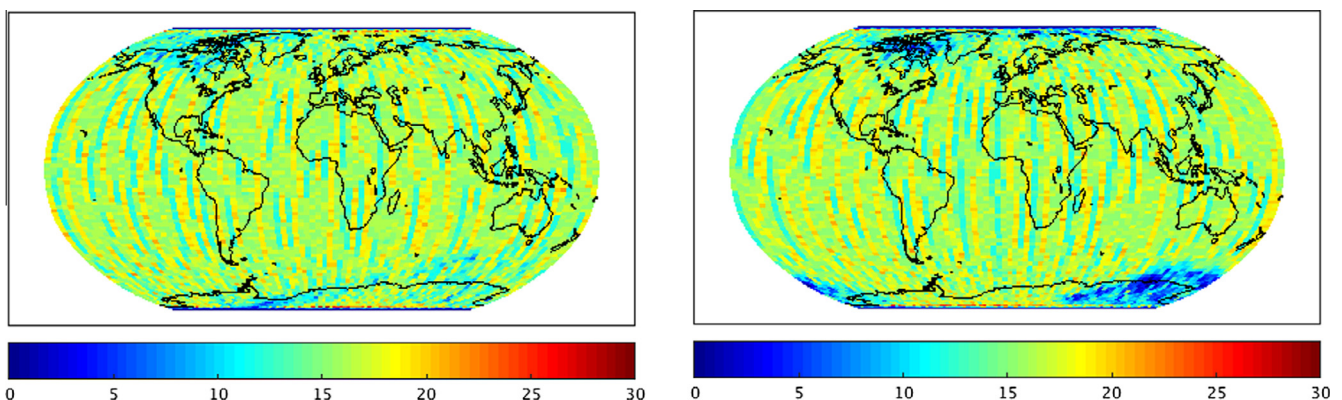


Fig. 13. Number of kinematic Swarm-A positions for ascending (left) and descending (right) arcs in March 2014.

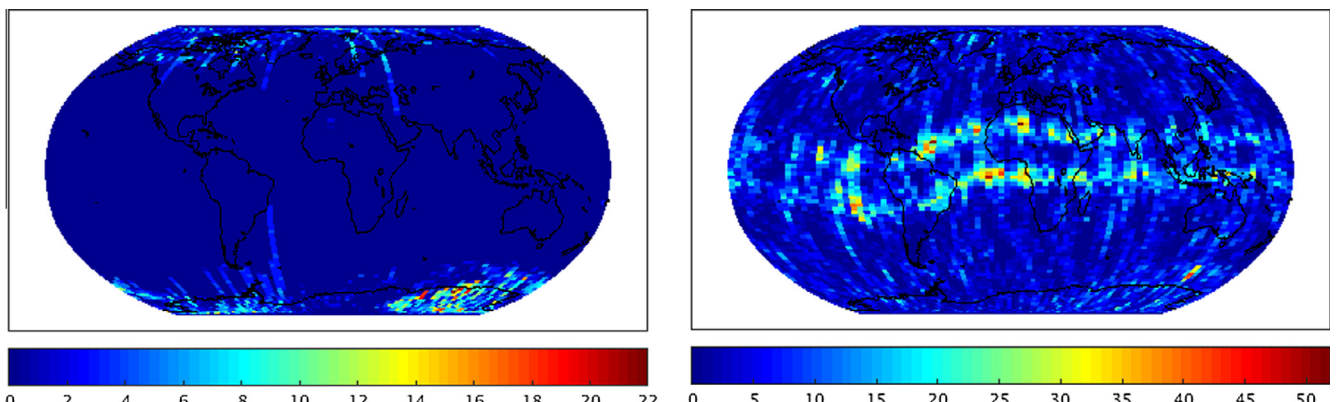


Fig. 14. Number of missing GPS carrier phase data on both frequencies for Swarm-A (left) and GRACE-B (right) for all arcs in March 2014.

3.5. Time-variability

The GRACE mission is currently the only dedicated gravity mission in orbit to map the Earth's time-variable gravity field by ultra-precise inter-satellite K-band ranging (Tapley et al., 2004). In view of the possibility of a potential failure of the GRACE spacecraft in the near future, Satellite Laser Ranging to spherical satellites (e.g., Sosnica et al., 2015) and/or GPS high-low SST of non-dedicated satellites (e.g., Weigelt et al., 2013) might play an important role to

bridge the gap between the current GRACE and the future GRACE Follow-On mission (Flechtner et al., 2013). The Swarm mission is one of the candidate missions to contribute to the recovery of time-variable gravity signals from GPS high-low SST.

Although the Swarm time series is currently only covering 18 months and thus still too short for a very detailed analysis, a first glimpse on Swarm's capability to recover time-variable gravity signals can already be got by comparing monthly Swarm solutions with those from GRACE

K-band ranging over regions with strong time-variable gravity signals. Fig. 15 compares the time-variable signal over the Amazon basin in equivalent water heights as obtained from the GFZ RL05a GRACE monthly solutions (Dahle et al., 2012) and from the monthly recoveries from Swarm-A, -B, -C, and the combination of all Swarm satellites, respectively. The Swarm solutions are 500 km Gauss filtered to focus on the long-wavelength information. For comparability the GRACE solutions are 500 km Gauss filtered, as well, but also DDK5 filtered (Kusche, 2007) to additionally display the “true”, i.e., less affected by signal damping, gravity signal of the Amazon basin. For all comparisons the GOCO05S static field and trend coefficients (evaluated on 01 September 2014) are subtracted. Fig. 15 shows that the annual signal is well recovered by the Swarm satellites, especially from Swarm-C. Only two obvious outliers are observed for the Swarm-C solutions of December 2013 and January 2014, i.e., before the satellite was maneuvered to its lower orbital altitude. A similar performance is also observed for Swarm-A, but some additional outliers are present. A generally worse performance is observed for the higher flying Swarm-B satellite. Due to

these outliers also the combination is currently still worse than the solution obtained from Swarm-C. Although further investigations are needed to explain the cause of the outlying monthly solutions, a clear sensitivity to the largest time variable gravity signal of the Amazon basin can be assessed. As soon as the Swarm time series will be longer, model fits may also be performed to further improve the recovery of the seasonal signal.

4. Outlook on Swarm baseline determination

The close formation of Swarm-A and -C also offers the additional possibility to directly determine the difference vector between the two satellites (space baseline) in the reduced-dynamic or kinematic mode from differential GPS. The potential benefit of using millimeter precise kinematic space baselines for gravity field determination has not yet been widely investigated with real space baseline data, e.g., from GRACE (Jäggi et al., 2009a), and might be of particular interest for gravity field recovery from Swarm. As opposed to GRACE, the close formation of Swarm-A and -C is not only separated in the along-track

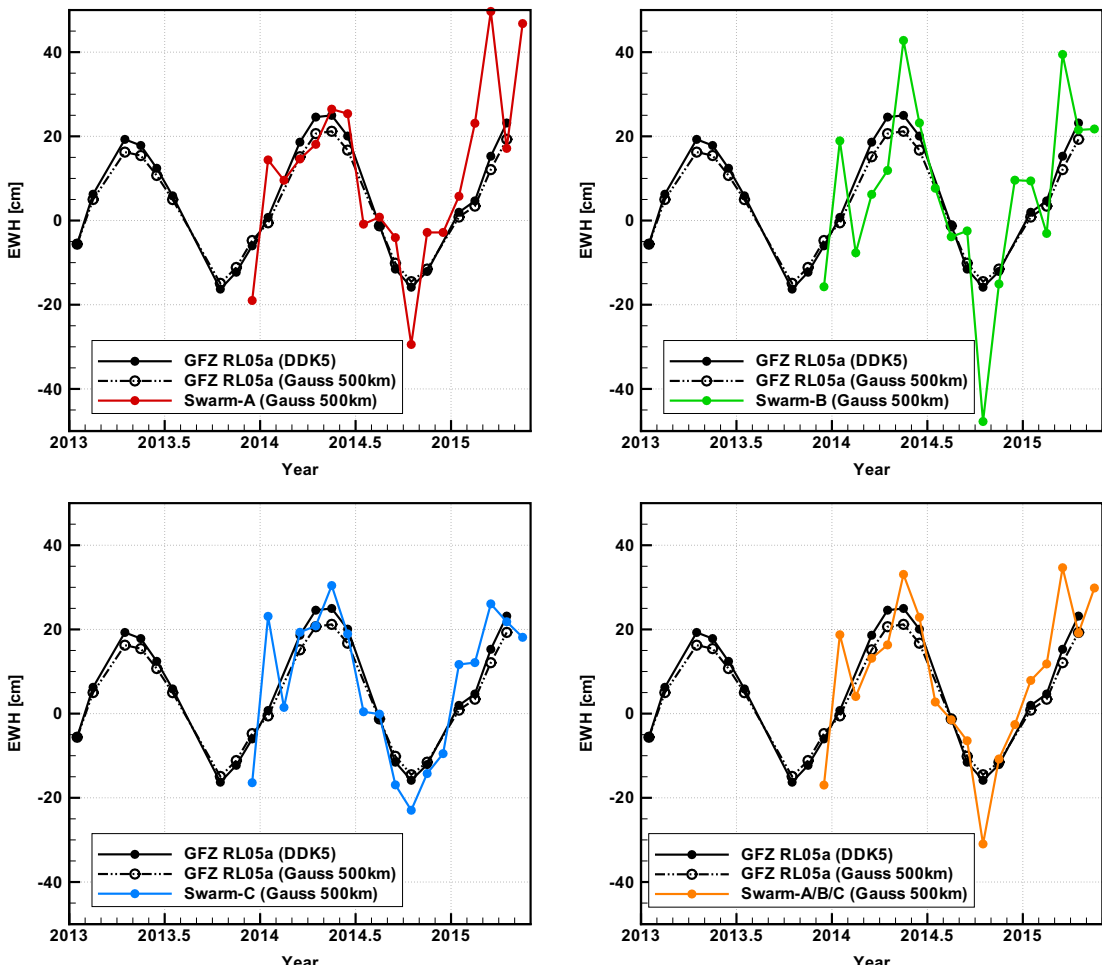


Fig. 15. Filtered time variable gravity signal over the Amazon basin derived from GRACE and from monthly recoveries from Swarm-A (top, left), Swarm-B (top, right), Swarm-C (bottom, left), and from the combination of all Swarm satellites (bottom, right).

direction, but also in cross-track direction with maximum separation at equator crossings. Differential GPS requires concurrent observations on Swarm-A and -C, which were available at 10-s sampling since 1 March 2014 and at 1-s sampling since 15 July 2014. Because the fractional parts of the observation epochs for the Swarm satellites do not differ by more than 0.2 μ s (van den IJssel et al., 2015) in the worst case, this only translates in a phase modeling error of about 1.6 mm at maximum due to the satellites' orbital velocity. The level of clock synchronization is therefore sufficient to enable differential GPS between Swarm-A and -C without a need to interpolate observations to a common epoch.

For a very first assessment of Swarm kinematic and reduced-dynamic baseline determination the same procedures are used as for GRACE (Jäggi et al., 2007) and TerraSAR-X/TanDEM-X (Jäggi et al., 2012) baseline determination. The positions of one satellite (Swarm-A) are kept fixed to a reduced-dynamic solution based on undifferenced ionosphere-free GPS carrier phase observations. Reduced-dynamic orbit parameters or kinematic positions of the other satellite (Swarm-C) are then estimated by processing double-difference (DD) ionosphere-free GPS carrier phase observations with DD ambiguities resolved to their integer values. For this purpose, the Melbourne-Wübbena linear combination is analyzed first to resolve the wide-lane ambiguities, which are subsequently introduced as known to resolve the narrow-lane ambiguities together with the reduced-dynamic or the kinematic baseline determination. As opposed to the receivers onboard the GRACE and TanDEM-X missions, the Swarm GPS receivers are known to generate GPS carrier phase measurements also with half-cycle ambiguities (M. Sust, personal communication), which has to be considered in the analysis. For a first assessment this has been ignored, however, because for a one month test period a very high number (about 97%) of the wide-lane ambiguities could indeed be resolved to integer numbers (Jäggi et al., 2014). Due to the very large wide-lane wavelength of about 86.2 cm this indicates that at least the wide-lane ambiguities are full cycle ambiguities even though this has not yet been confirmed through the receiver design. Note that this implies that the L_1 and L_2 ambiguities are either both half cycle or both full cycle ambiguities with no mixing of full and half cycle ambiguities on the L_1 and L_2 carriers. Interestingly, also a substantial number of narrow-lane ambiguities (about 89%) is fixed to full cycle ambiguities (Jäggi et al., 2014). This might, however, also include a number of wrong fixes due to the very short narrow-lane wavelength of only about 10.7 cm.

In order to illustrate the main issue that needs to be resolved before kinematic Swarm baselines may be successfully tested as a new observable for gravity field determination, Fig. 16 shows the currently achieved quality of a kinematic Swarm baseline solutions for one particular day in comparison to a kinematic baseline solution with proven quality obtained from one day of GRACE GPS

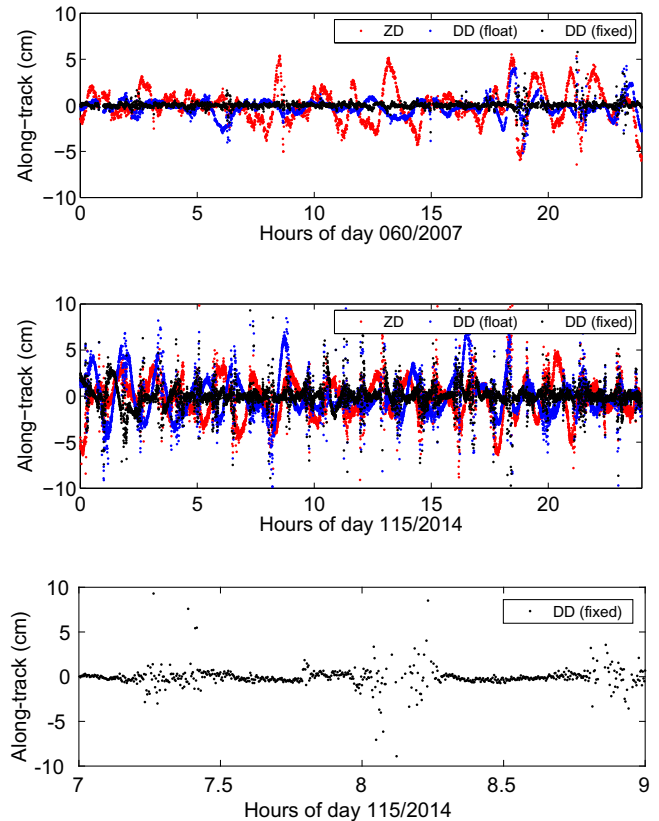


Fig. 16. Differences between kinematic and reduced-dynamic positions of GRACE-B (top), Swarm-C (middle), and zoom on the Swarm-C baseline differences (bottom).

data. For all solutions shown in Fig. 16 the positions of the first satellite (GRACE-A, Swarm-A) are kept fixed to their respective reduced-dynamic solution based on undifferenced GPS data. For the second satellite (GRACE-B, Swarm-C) both reduced-dynamic and kinematic positions are computed by following three different approaches: undifferenced GPS data processing, doubly differenced GPS data processing without ambiguity fixing, and doubly differenced GPS data processing with ambiguity fixing. For all three cases the differences between the respective kinematic and reduced-dynamic solutions are shown in Fig. 16 for the along-track direction of GRACE-B (top) and of Swarm-C (middle, bottom), respectively. The figures illustrate that the ambiguity fixing successfully removes for both constellations once-per-revolution like signatures, as was already illustrated for GRACE by Jäggi et al. (2009a). To a large extent this works fine for Swarm, as well, although it cannot be excluded that some of the remaining variations are caused by wrong fixes due to the half cycle issue mentioned above. More importantly, however, Fig. 16 (middle) reveals the presence of significant excursions occurring twice per revolution, which take place over the geomagnetic poles. Fig. 16 (bottom) provides a zoom on two hours and confirms that the kinematic positions are significantly degraded even in the case of ambiguity fixing. Due to the rather long validity intervals

of the ambiguities this most probably also impacts the kinematic positions outside the polar regions and asks for tailored ambiguity resolution procedures taking into account the significantly different GPS data quality over the polar regions and outside.

5. Summary

Swarm kinematic positions have been generated at AIUB since 25 November 2013 for all Swarm satellites using different releases of GPS data. Virtually the same orbit quality is achieved for the different releases thanks to an individual in-flight calibration of the Swarm GPS antenna phase center variations. Using the latest release of GPS data the independent validation of the kinematic orbits with SLR data shows a very good quality of 3.25, 2.74, and 3.11 cm SLR RMS errors for Swarm-A, -B, and -C, respectively. Mean SLR offsets are found to be small with values of 0.27, 0.10, and 0.06 cm, respectively. The analysis of GPS carrier phase residuals revealed a clear geographical dependency. Significantly larger residuals occur over the geomagnetic poles, but are of excellent quality elsewhere. The magnitude of the residuals is correlated with the ionosphere activity documented by the mean daily TEC.

Based on the kinematic positions gravity field determination was performed using the Celestial Mechanics Approach. Long-term solutions based on data from 1 December 2013 up to 31 December 2014 and up to 27 May 2015, respectively, and solutions based on bi-monthly periods inside the year 2014 were generated. All solutions were affected by severe systematic errors along the geomagnetic equator. Due to the changing orbit geometry and the varying ionosphere activity the size of the systematic errors is significantly changing, as well. Barely visible for the June–July period, the maximum impact occurs for February–April and September–December, which also correlate with ionosphere activity.

Similarly to the findings for the GOCE mission, kinematic positions related to situations with large ionospheric changes are found to be responsible for the observed artifacts in the gravity field solutions. Rejecting GPS data with ionospheric changes larger than 2 cm/s leads to a reduction of the useable GPS observations of at maximum 10% for kinematic orbit determination during periods with severe ionosphere conditions, but, more importantly, results in a significant reduction of the systematic errors in the gravity field recovery. No degradation was found for the static solutions when rejecting GPS data with large ionospheric changes, but for the bi-monthly solutions a small degradation had to be noted for degrees below 10 in the presence of severe ionosphere conditions. Either a more refined screening or an improved modeling of the HOI correction terms should therefore be developed to further minimize the amount of rejected GPS data.

The static gravity fields from Swarm were compared with corresponding solutions from GRACE using only GPS data. The GRACE solutions do not show artificial

signatures along the geomagnetic equator, because the critical GPS data is not present in the GPS observation files. The low degree coefficients recovered from Swarm up to about degree 20 turned out to be of a similar quality as those from GRACE when rejecting GPS data with large ionospheric changes for Swarm. Swarm will therefore be equally well suited to derive the long wavelength time-variable gravity field signals as GRACE GPS data can do. A first glimpse on the Amazon basin indeed confirmed the sensitivity of Swarm to the largest time-variable signals. For the higher degrees, however, the Swarm solutions are inferior to GRACE GPS-only solutions due to higher orbital altitude and the higher noise in the GPS data.

Eventually, a first set of kinematic baselines between the Swarm-A and Swarm-C satellites has been generated. Despite the potential presence of half cycle ambiguities, a significant number of carrier phase ambiguities could be fixed to integer (full cycle) ambiguities and typical once-per-revolution patterns between the kinematic and reduced-dynamic solutions could be reduced. This first glance at the quality of kinematic Swarm baselines also confirmed, however, that the issues with the Swarm GPS data over polar regions are problematic to generate proper baseline solutions over 24 h arcs. A potential improvement might be expected from the side of the instrument by adjusting the settings of the receiver tracking loops, as performed on 6 May 2015 for Swarm-C, but more research is required to further improve the kinematic Swarm baselines also from the side of the analysis, e.g., by adopting tailored weighting schemes for the problematic GPS data over the polar regions, such that they may be used as a new observable for gravity field determination.

The Swarm kinematic orbits are available via the AIUB anonymous ftp server ftp://ftp.unibe.ch/aiub/LEO_ORBITS/.

Acknowledgments

This work was partly performed in the framework of the Swarm Quality Working Group (QWG), which is organized by ESA. C. Dahle has been funded by the German Federal Ministry of Education and Research (BMBF) with support code 03F0654A. Helpful discussions with Christian Siemes, Oliver Montenbruck, and Franz Zangerl are kindly acknowledged.

References

- Basu, S., Groves, K.M., 2001. Specification and forecasting of outages on satellite communication and navigation systems. In: Song, P., Singer, H.J., Siscoe, G.L. (Eds), Space weather geophysical monograph series, vol. 125, pp. 424–430, <http://dx.doi.org/10.1029/GM125p0423>.
- Beutler, G., Jäggi, A., Mervart, L., et al., 2010. The celestial mechanics approach: theoretical foundations. *J. Geod.* 84 (10), 605–624. <http://dx.doi.org/10.1007/s00190-010-0401-7>.
- Bock, H., Dach, R., Jäggi, A., et al., 2009. High-rate GPS clock corrections from CODE: support of 1 Hz applications. *J. Geod.* 83 (11), 1083–1094. <http://dx.doi.org/10.1007/s00190-009-0326-1>.

- Bock, H., Jäggi, A., Beutler, G., et al., 2014. GOCE: precise orbit determination for the entire mission. *J. Geod.* 88 (11), 1047–1060. <http://dx.doi.org/10.1007/s00190-014-0742-8>.
- Buchert, S., Zangerl, F., Sust, M., et al., 2015. Swarm observations of equatorial electron densities and topside GPS track losses. *Geophys. Res. Lett.* 42, 2088–2092. <http://dx.doi.org/10.1002/2015GL063121>.
- Dach, R., Hugentobler, U., Fridez, P. (Eds.), 2007. Bernese GPS Software Version 5.0. Documentation. Astronomical Institute University of Bern, Bern.
- Dach, R., Brockmann, E., Schaer, S., et al., 2009. GNSS processing at CODE: status report. *J. Geod.* 83 (3–4), 353–365. <http://dx.doi.org/10.1007/s00190-008-0281-2>.
- Dach, R., Schaer, S., Lutz, S., et al., 2014. Center for orbit determination in Europe: IGS technical report 2013. In: Dach, R., Jean, Y. (Eds.), International GNSS Service: Technical Report 2013. IGS Central Bureau, pp. 21–34.
- Dahle, C., Flechtner, F., Gruber, C., et al., 2012. GFZ GRACE Level-2 Processing Standards Document for Level-2 Product Release 0005, Scientific Technical Report STR12/02 – Data, Revised Edition, January 2013. <http://dx.doi.org/10.2312/GFZ.b103-1202-25>.
- Dunn, C., Bertiger, W., Bar-Sever, Y., et al., 2003. Instrument of GRACE. *GPS World*.
- Flechtner, F., Morton, P., Watkins, M., et al., 2013. Status of the GRACE follow-on mission. In: Marti, U. (Ed), Gravity, Geoid and Height Systems. IAG Symposia 141, pp. 117–121. http://dx.doi.org/10.1007/978-3-319-10837-7_15.
- Friis-Christensen, E., Lühr, H., Knudsen, D., et al., 2008. Swarm – an earth observation mission investigating geospace. *Adv. Space Res.* 41 (1), 210–216. <http://dx.doi.org/10.1016/j.asr.2006.10.008>.
- Jäggi, A., Hugentobler, U., Beutler, G., 2006. Pseudo-stochastic orbit modeling techniques for low-Earth orbiters. *J. Geod.* 80 (1), 47–60. <http://dx.doi.org/10.1007/s00190-006-0029-9>.
- Jäggi, A., Hugentobler, U., Bock, H., et al., 2007. Precise orbit determination for GRACE using undifferenced or doubly differenced GPS data. *Adv. Space Res.* 39 (10), 1612–1619. <http://dx.doi.org/10.1016/j.asr.2007.03.012>.
- Jäggi, A., Beutler, G., Prange, L., et al., 2009a. Assessment of GPS-only observables for gravity field recovery from GRACE. In: Sideris, M.G., (Ed). Observing our Changing Earth. IAG Symposia 133. pp. 113–123. http://dx.doi.org/10.1007/978-3-540-85426-5_14.
- Jäggi, A., Dach, R., Montenbruck, O., et al., 2009b. Phase center modeling for LEO GPS receiver antennas and its impact on precise orbit determination. *J. Geod.* 83 (12), 1145–1162. <http://dx.doi.org/10.1007/s00190-009-0333-2>.
- Jäggi, A., Bock, H., Prange, L., et al., 2011a. GPS-only gravity field recovery with GOCE, CHAMP, and GRACE. *Adv. Space Res.* 47 (6), 1020–1028. <http://dx.doi.org/10.1016/j.asr.2010.11.008>.
- Jäggi, A., Prange, L., Hugentobler, U., 2011b. Impact of covariance information of kinematic positions on orbit reconstruction and gravity field recovery. *Adv. Space Res.* 47 (9), 1472–1479. <http://dx.doi.org/10.1016/j.asr.2010.12.009>.
- Jäggi, A., Montenbruck, O., Moon, Y., et al., 2012. Inter-agency comparison of TanDEM-X baseline solutions. *Adv. Space Res.* 50 (2), 260–271. <http://dx.doi.org/10.1016/j.asr.2012.03.027>.
- Jäggi, A., Dahle, C., Arnold, D., et al., 2014. Kinematic space-baselines and their use for gravity field recovery. In: Presented at the 40th COSPAR Scientific Assembly, Moscow, Russia.
- Jäggi, A., Bock, H., Meyer, U., et al., 2015. GOCE: assessment of GPS-only gravity field determination. *J. Geod.* 89 (1), 33–48. <http://dx.doi.org/10.1007/s00190-014-0759-z>.
- Kusche, J., 2007. Approximate decorrelation and non-isotropic smoothing of time-variable GRACE-type gravity field models. *J. Geod.* 81 (11), 733–749. <http://dx.doi.org/10.1007/s00190-007-0143-3>.
- Lyard, F., Lefevre, F., Letellier, T., et al., 2006. Modelling the global ocean tides: insights from FES2004. *Ocean Dyn.* 56, 394–415. <http://dx.doi.org/10.1007/s10236-006-0086-x>.
- Mayer-Gürr, T. et al., 2015. The combined satellite gravity field model GOCO05S. *Geophys. Res. Abs.* 17.
- Olsen, N., Friis-Christensen, E., Floberhagen, R., et al., 2013. The Swarm Satellite Constellation Application and Research Facility (SCARF) and Swarm data products. *Earth Planets Space* 65 (11), 1189–1200. <http://dx.doi.org/10.5047/eps.2013.07.001>.
- Pavlis, N.K., Holmes, S.A., Kenyon, S.C., et al., 2012. The development and evaluation of the Earth Gravitational Model 2008 (EGM2008). *J. Geophys. Res.* 117, B04406. <http://dx.doi.org/10.1029/2011JB008916>.
- Pearlman, M.R., Degnan, J.J., Bosworth, J.M., 2002. The International laser ranging service. *Adv. Space Res.* 30 (2), 135–143. [http://dx.doi.org/10.1016/S0273-1177\(02\)00277-6](http://dx.doi.org/10.1016/S0273-1177(02)00277-6).
- Petit, G., Luzum, B., 2010. IERS Conventions 2010. IERS Technical note no.36. Bundesamt für Kartographie und Geodäsie, Frankfurt am Main, Germany.
- Sośnicka, K., Jäggi, A., Meyer, U., et al., 2015. Time variable Earth's gravity field from SLR satellites. *J. Geod.* 89 (10), 945–960. <http://dx.doi.org/10.1007/s00190-015-0825-1>.
- Sust, M., Zangerl, F., Montenbruck, O., et al., 2014. Spaceborne GNSS-Receiving System Performance Prediction and Validation. In: NAVITEC 2014, ESA Workshop on Satellite Navigation Technologies and GNSS Signals and Signal Processing, 3–5 Dec 2014, Noordwijk, The Netherlands.
- Švehla, D., Rothacher, M., 2005. Kinematic precise orbit determination for gravity field determination. In: Sansò, F., (Ed). A window on the future of geodesy. IAG Symposia 128, pp. 181–188, http://dx.doi.org/10.1007/3-540-27432-4_32.
- Tapley, B.D., Bettadpur, S., Ries, J.C., et al., 2004. GRACE measurements of mass variability in the Earth system. *Science* 305 (5683), 503–505. <http://dx.doi.org/10.1126/science.1099192>.
- van den IJssel, J., Encarnaçao, J., Doornbos, E., et al., 2015. Precise science orbits for the Swarm satellite constellation. *Adv. Space Res.* 56 (6), 1042–1055. <http://dx.doi.org/10.1016/j.asr.2015.06.002>.
- Weigelt, M., van Dam, T., Jäggi, A., et al., 2013. Time-variable gravity signal in Greenland revealed by high-low satellite-to-satellite tracking. *J. Geophys. Res. Solid Earth* 118 (7), 3848–3859. <http://dx.doi.org/10.1002/jgrb.50283>.
- Wu, S.C., Yunck, T.P., Thornton, C.L., 1991. Reduced-dynamic technique for precise orbit determination of low Earth satellites. *J. Guid. Control Dyn.* 14 (1), 24–30.
- Wu, S.C., Kruizinga, G., Bertiger, W., 2006. Algorithm Theoretical Basis Document for GRACE Level-1B Data Processing V1.2, D-27672. JPL Publication, Pasadena, California.
- Zangerl, F., Griesauer, F., Sust, M., et al., 2014. SWARM GPS precise orbit determination receiver initial in-orbit performance evaluation. In: Proceedings of the 27th International Technical Meeting of the Satellite Division of the Institute of Navigation (ION GNSS+). pp. 1459–1468. Tampa, Florida.
- Zumberge, J.F., Heflin, M.B., Jefferson, D.C., et al., 1997. Precise point positioning for the efficient and robust analysis of GPS data from large networks. *J. Geophys. Res.* 102 (B3), 5005–5017. <http://dx.doi.org/10.1029/96JB03860>.